3D Reconstruction of peripheral nerves from optical projection tomography (OPT) images. A method for studying fascicular interconnections and intraneural plexuses

ABSTRACT 234 words

Background: The general microscopic characteristics of nerves are described in several textbooks of histology, but the specific microanatomies of most nerves that can be blocked by anesthesiologists are usually less well known.

Our objective was to evaluate the 3D reconstruction of nerve fascicles from optical projection tomography images (OPT) and the ability to undertake an internal navigation exploring the morphology in detail, more specifically the fascicular interconnections.

Methods: Median and lingual nerve samples were obtained from five euthanized piglets. OPT images of the samples were acquired and 3D reconstruction was performed.

Results: The OPT technique revealed the inner structure of the nerves at high resolution, including large and small fascicles, perineurium, interfascicular tissue and epineurium. The fascicles were loosely packed inside the median nerve and more densely so in the lingual nerve.

Analysis of the 3D models demonstrated that the nerve fascicles can show six general spatial patterns. Fascicular interconnections were clearly identified.

Conclusions: The 3D reconstruction of nerve fascicles from OPT images opens a new path for research into the microstructure of the inner contents of fascicular nerve groups and their spatial disposition within the nerve including their interconnections.

These techniques enable 3D images of partial areas of nerves to be produced and could became an excellent tool for obtaining data concerning the 3D microanatomy of nerves, essential for better interpretation of ultrasound images in clinical practice and thus avoiding possible neurological complications.

KEY WORDS: 3D reconstructions, optical projection tomography, peripheral nerve, fascicles.

INTRODUCTION 492 words

The use of ultrasonography in clinical practice has increased the interest of anesthesiologists in acquiring more detailed knowledge of the internal structures of nerves examined under the ultrasound probe. The general microscopic characteristics of nerves are described in several textbooks of histology, but the specific microanatomies of most nerves that can be blocked by anesthesiologists are less well known.

Several questions about the microanatomy of nerves can arise, such as the possible reasons why nerves maintain special arrangements rather than more random distributions of internal groups of fascicles (Reina et al., 2013; Reina et al., 2015a,b). Isolated or in groups, nerve fascicles form topograms (maps of fascicles) that can be seen in cross-sections of nerves. The question is: why are these topograms similar when studied in the same region of the same nerve in different cadavers (Reina et al.,2015a)? Our aim is to identify factors that could contribute to keeping these fascicles tightly together in their groups.

Six decades ago, Sunderland (1945; 1948; 1949; 1959) studied the internal arrangements of fascicles and the intraneural plexuses formed by interconnections among neighboring fascicles. He illustrated his results with diagrams giving three-dimensional portrayals of those intraneural plexuses. These studies were not continued by other researchers. Nowadays, modern high resolution ultrasonography enables fascicular groups to be identified by placing the tip of the needle within them, showing how nerve fascicles could be separated after an injection of local anesthetic.

In order to demonstrate the existence of fascicular interconnections inside nerves that are often blocked, care must be taken to avoid breaking these little fascicles during local anesthetic injection into fascicular groups, thus preventing serious neurological complications.

Histological cross-section allows us to study structures such as these and their significant aspects. However, 3D image reconstruction provides a unique way of examining fascicular patterns and are necessary for finding the explanation for the consistent fascicular nerve disposition. Three-dimensional reconstructions from histological slides are technically very difficult at high magnification, leading to errors related to the methods used during preparation of the cross-section slides. Errors arise especially from deformations caused by physical cutting, missing information due to cut-off, or loss or destruction of some cross-sections.

Optical projection tomography (OPT) (Sharpe, 2003) is a new method for studying microstructures in 3D. This method enables us to obtain digital images containing fine details of the fascicles within the nerve, including small fascicles about 10-15 mm in length along the nerve, producing spatial data that provide information similar to that obtained with magnetic resonance images (MRI) but at higher resolution (circa 10 times; a voxel of about 0.6 mm from MRI vs. approximately 60 μm from OPT).

Our group applied the OPT technique to study lesions of the nerve caused during anesthetic nerve blockades (Cvetko, 2015). In addition, 3D reconstructions of the lumbar spine and its internal nervous structures were obtained from MRI (Puigdellívol-Sánchez et al., 2011; Prats-Galino et al., 2012; Prats-Galino et al., 2014; Prats-Galino et al., 2015; Reina et al., 2016). Our objective was to evaluate the 3D reconstruction of nerve fascicles from OPT images and the ability to undertake an internal navigation exploring the morphology in detail, more specifically the fascicular interconnections.

METHODS

Ten nerve samples were obtained from five euthanized piglets (animals that had been used in another protocol) as approved by Institutional Review Board for Animal Research No U34401-28/2013/7. As previously described (Cvetko al., 2015), after deep intramuscular sedation (midazolam 0.5 mg kg^{-1}, ketamine 10 mg kg^{-1} and butorphanol 0.5 mg kg^{-1}), an intravenous line was inserted and anesthesia induced using 1-2 mg kg^{-1} propofol. During deep anesthesia, the piglets received 3 ml per 10 kg T61 euthanasia solution (1 ml contains embutramid 200 mg, mebezonium iodide 50 mg and tetracaine hydrochloride 5 mg; Hoechst GmbH, Frankfurt-Hochst, Germany).

The axillary region was dissected to expose the median nerve (n=5) and the infratemporal region was dissected to expose the lingual nerve (n=5). The nerves were excised and fixed in 100% methanol at 4 °C for 48 h. The nerve samples were then dehydrated over 24 h through three washes of 100% methanol and finally cleared for 24 h in BABB (1 part benzyl alcohol to 2 parts benzyl benzoate), allowing the remaining alcohol to evaporate.

Optical Projection Tomography Acquisition

OPT images of the nerve samples were acquired using a custom-made OPT machine developed in cooperation with the Politecnico di Milano, Italy (Bassi, 2015) and installed in the Institute of Physiology CAS in Prague. Compared to the commercial OPT 3001 scanner made by Bioptonics, Edinburgh, UK (Bioptonics, 2015), which is no longer produced, the machine is equipped with a more sensitive camera and more precise Plan Apo Infinity-Corrected objectives (2x, 5x,10x), giving images of higher quality.

The images were acquired using excitation at 405 nm and fluorescence emissions were captured at 550 nm with a high pass filter. For each specimen, 400 image projections, obtained with a step of 0.9 degrees and a resolution of 1004 x 1004 pixels per projection, were captured and coded at 16 bits per pixel. Since the nerve specimens were large, we used an OPT setup with a low magnifying 2x objective lens that provided the pixel size in the projections of 5.42 x 5.42 μm^2. Tomographic reconstructions were subsequently created using the free software package NRecon (Bruker, 2014). The resulting reconstructed stack contained about one thousand axial images.

3D Reconstruction

Axial OPT images were exported as a sequence of bmp files, which were imported as a single image volume (stack) for analysis using Amira v5.6 3D software (Mercury Co, Boston, MA) installed in a Dell Precision graphic station at the Laboratory of Surgical NeuroAnatomy (LSNA), University of Barcelona. This software is designed for visualization and analysis of biomedical images, allowing volumetric reconstructions to be produced.

To generate the 3D models from each image volume the following steps were performed (Fig 1): (1) semiautomatic segmentation of the whole nerve and its fascicles, resulting in two Volumes of Interest (VOIs); (2) manual correction of the VOIs by a 3D editor; (3) identification of individual nerve fascicles, assigning a different VOI to each; (4) surface generation by triangulation of VOIs and reduction of the number of triangles to simplify the meshes; (5) automatic smoothing of the models; and (6) quality checking of the 3D models generated. Steps 2-6 were repeated until a clear correspondence between each model contour and its corresponding structure in the OPT images was obtained. Both ends of the nerves were excluded from the reconstruction because of the greater frequency of artifacts and geometrical distortions in those regions.

RESULTS

The OPT technique showed the inner structure of the nerve at high resolution, including large and small fascicles, perineurium, interfascicular tissue and epineurium (Fig. 1). The triangular meshes generated from the different reconstructed structures reached a resolution of 0.005 mm^2 per triangle.

The nerve fascicles were loosely packed inside the median nerve (Fig. 2) and more densely in the lingual nerve (Fig. 3). In the lingual nerve, the perineurium of most of the fascicles was attached to the epineurium with very little interfascicular tissue (fat). In contrast, in the median nerve, nerve fascicles remained separated by abundant amounts of fat tissue delimiting two large fascicular groups and a smaller group. The fascicles were helical, more evidently in the median than the lingual nerves.

Analysis of the 3D models demonstrated that the nerve fascicles can show six general spatial patterns: (1) isolated fascicle pattern, a single nerve fascicle with no relationship to other adjacent fascicles (Fig. 4a); (2) confluent or "Y-shape" pattern, in which two fascicles usually converge to form a single one (Fig.5a); (3) bifurcating or "inverted Y-shape" pattern, with a diverging configuration (Fig. 4b); (4) crossing or "X-shape" pattern (Fig. 5b); (5) fascicular interconnection, thin bridges connecting two nerve fascicles (Fig. 6a); and (6) complex interconnection, resulting from a variable combination of the previous patterns in the segment of the nerve analyzed (Fig. 6b).

Fascicular interconnections were clearly identified after 3D reconstruction in the median nerve, showing a lower size limit of 60 μm diameter in our samples.

DISCUSSION 1276 words

The 3D reconstruction of nerve fascicles from OPT images opens a new path for research into the microstructures of peripheral nerves, which proved adequate owing to the high resolution of the technique. OPT enables the internal structures of nerves to be studied in large samples about 1 to 12 mm in diameter and 10-15 mm in length at microscale resolution. This technique navigates through substantially small structures, facilitating dynamic analysis and image capture that reveals fine details from the inner structure of the nerve under examination. OPT is therefore a good tool for identifying differences between the two nerves in terms of their diameters and in the number and morphological aspects of their fascicles. Also, measurements of the ratio of neural to non-neural tissue can be checked along large samples of the nerve, although the latter data can be obtained more precisely and directly from cross-section histological slides.

The most important difference between OPT and other techniques is its ability to check minute details of the internal structure of the nerve in large samples as it can navigate inside the nerve while providing 3D images. This technique offers the possibility of alternatively showing or hiding 3D reconstruction structures in order to focus on specific areas.

The OPT technique enables our knowledge regarding ultrastructural details of the inner contents of fascicular nerve groups to be broadened and their spatial disposition within the nerve including their interconnections to be established. This knowledge could contribute to understanding the mechanisms leading to nerve injury and neurological complications caused by peripheral and regional anesthetic blocks. The location of the tip of the needle on the outer or inner side of the nerve is fundamental to the possible cause of nerve injury leading to neurological complications after anesthetic blocks.

Concerns regarding intrafascicular and extrafascicular placement of local anesthetic solutions are as well known as the different neurological consequences that can ensue (Sala-Blanch et al., 2011a; Sala-Blanch et al., 2013). Intrafascicular injections cause an increase of pressure (Hadzic et al., 2004), which can affect the axons and induce capillary collapse, and also tear the perineurium causing loss of the normal intrafascicular pressure necessary for adequate axon function. The axons are injured by mechanical forces affecting several of them, and intrafascicular lesions of arteries, venules and capillaries with different degrees of intrafascicular hemorrhage and later fibrosis also affect the normal functioning of axons (Brull et al., 2015).

.

In contrast, extrafascicular injection does not produce neurological complications when the local anesthetic volume is injected between two large groups of nerve fascicles, such as the sciatic nerve at popliteal level (Sala-Blanch et al., 2011b). However, this nerve at this level shows specific structural features and conclusions drawn from findings concerning it cannot be extrapolated to other nerves. Therefore, it cannot serve as a standard model of the possible consequences during extrafascicular injection. Most nerves have extrafascicular tissue (interfascicular tissue is formed mainly by fat) similar in size and relationship to those found among the fascicles inside fascicular groups such as the afore mentioned sciatic nerve. Conversely, in the sciatic nerve as a whole, fat between the two large groups of fascicles remains as paraneural fat, which can be found on the outer side in other nerves and on the outer side of the cords of the brachial plexus. One objective of this study is to draw attention to the fact that nerve fascicles within a group generally join together and appear surrounded by fat (Reina et al., 2015a).

Small amounts of fat among the fascicles are commonly observed. This pattern is similar in most nerves. OPT 3D reconstruction has demonstrated these features through 3D reconstruction images obtained while navigating along the fascicles. Therefore, the presence of fascicular interconnections can be ascertained, which explain the short distances among groups of nerve fascicles and their particular spatial arrangements.

Three-dimensional reconstructions from OPT images represent a new approach to investigating nerve fascicles, their arrangement into groups, their merging and diverging, and the fascicular interconnections among them. Probably the number, size and angle of those fascicular interconnections act as forces that maintain the nerve fascicles and join them together into groups. All delicate structures form the intraneural plexus studied by Sunderland (1945; 1948; 1949; 1959) and could be checked perfectly nowadays in all nerves by OPT 3D reconstructions.

Knowledge of the internal microanatomies of nerves regarding anesthetic blockade could help prevent possible neurological complications (Brull et al., 2015). The intraneural extrafascicular injection technique, where local anesthetic is injected within a group of fascicles, is frequently advocated (Sala-Blanch et al., 2009), and the ultrasound technique allows us to see how fascicles become separated after a local anesthetic volume is injected. However, ultrasound images have insufficient image resolution to depict fascicular interconnections so it has been assumed that fascicles are independent structures kept together by external coverings.

Conversely, extrafascicular injection of local anesthetic affects interconnections among nerve fascicles, which can be stretched and torn apart leading to loss of axons.

The helical shape of fascicles helps us understand how nerves can be stretched without excessive traction being exerted on them, providing natural protection against stretch forces during movement. This helical shape was apparent within the median nerve but almost absent in the lingual nerve, perhaps because the external protection of the jaw makes it unnecessary.

Visualization by the OPT microscope requires the tissue to be optically cleared to allow the light to pass through the object. A number of clearing protocols have been published recently; for reviews see (Kolesová et al., 2016; Tainaka et al., 2016; Azaripour et al., 2016).

We have experimented with BABB, Scale and CUBIC protocols for clearing nerve tissues. We reached the conclusion that BABB gives the best results from the point of view of transparency, although shrinkage of specimens can be a disadvantage. However, for the 3D reconstruction and modeling of fascicular interconnections described here, there were no important difficulties.

OPT acquisition is based on capturing optical projections of the specimen within a 360°scope and subsequent calculation of the 3D image using a tomographic reconstruction. Thus, the principle is similar to standard computed tomography, but instead of X-rays, OPT uses visible light. The maximum theoretical resolution of the OPT setup used is about 15 µm (with a 2x objective lens).

However, if the specimens are not perfectly cleared, non-uniform volume sampling is applied by rotating the specimen during the acquisition of projections, and non-ideal tomographic reconstruction is applied to projections to obtain 3D data. As a result, the theoretical resolution diminishes by a factor of 2-3 or even more in practice. Thus, OPT enables us to visualize fascicles at least 60 µm in diameter.

In future, detailed studies of several nerves under OPT 3D reconstruction could improve understanding of many dynamic ultrasound data obtained by anesthesiologists in real time, improving conclusions in our daily practice.

OPT 3D reconstruction images permit several details not currently revealed on the ultrasound device screens in our hospitals to be observed, because ultrasound devices have lower resolution than OPT 3D reconstruction. In future, data obtained from OPT 3D images will probably be displayed on the ultrasound device's screen amongst the fuzzy ultrasound image details.

In addition, data obtained from OPT 3D reconstruction will be useful to surgeons interested in nerve reconstruction as they could help to plan a surgical strategy.

The median and lingual nerve were studied as examples of different microanatomy types to evaluate the OPT 3D reconstruction technique, but other nerves would benefit from similar analysis by this technique. In future, it will be advisable to analyze new samples of human nerves in order to define all details of three-dimensional microarchitecture.

In summary, OPT DICOM files enable 3D images of partial areas of nerves to be produced and could became an excellent tool for obtaining data concerning the 3D microanatomy of nerves essential for better interpretation of ultrasound images during clinical practice, thus avoiding possible neurological complications.

REFERENCES

Azaripour A, Lagerweij T, Scharfbilig Ch, Jadczak AE, Willershausen B ,Van Noorden CJ. 2016. A survey of clearing techniques for 3D imaging of tissues with special reference to connective tissue. Progr Histochem Cytochem 51:9-23.

Bassi A. 2015. Optical projection tomography (OPT)
URL: http://www.fisi.polimi.it/en/research/research_structures/laboratories/50528 [accessed November 2017]

Bioptonics. 2015. Optical projection tomography. URL: http://www bioptonics.co.uk [accessed November 2017]

Bruker. 2014. Skyscanyscan, Software updates: Control and reconstruction programs. URL: http://www.skyscan.be/products/downloads.htm [accessed November 2017]

Brull R, Hadzic A, Reina MA, Barrington MJ. 2015. Pathophysiology and etiology of nerve injury following peripheral nerve blockade. Reg Anesth Pain Med 40:479-490.

Cvetko E, Čapek M, Damjanovska M, Reina MA, Eržen I, Stopar Pintarič T. 2015. Optical projection tomography: a new method for nerve micro-architecture 3D imaging. Anaesthesia 70:939-947.

Hadzic A, Dilberovic F, Shah S, Kulenovic A, Kapur E, Zaciragic A, Cosovic E, Vuckovic I, Divanovic KA, Mornjakovic Z, Thys DM, Santos AC. 2004. Combination of intraneural injection and high injection pressure leads to fascicular injury and neurologic deficits in dogs. Reg Anesth Pain Med 29:417-423.

Kolesová H, Čapek M, Radochová R, Janáček J, Sedmera D. 2016. Comparison of different tissue clearing methods and 3D imaging techniques for visualization of GFP- expressing mouse embryos and embryonic hearts. Histochem Cell Biol 146:141-152.

Prats-Galino A, Reina MA, Puigdellívol-Sánchez A, Juanes Méndez JA, De Andrés JA, Collier CB. 2012. Cerebrospinal fluid volume and nerve root vulnerability during lumbar puncture or spinal anaesthesia at different vertebral levels. Anaesth Intensive Care 40:643-647.

Prats-Galino A, Mavar M, Reina MA, Puigdellívol-Sánchez A, San-Molina J,

De Andrés JA. 2014. Three-dimensional interactive model of lumbar spinal structures.

Anaesthesia 69:521.

Prats-Galino A, Reina MA, Mavar Haramija M, Puigdellivol-Sánchez A, Juanes Méndez JA, De Andrés JA. 2015. 3D interactive model of lumbar spinal structures of anesthetic interest. Clin Anat 28:205-212.

Puigdellívol-Sánchez A, Prats-Galino A, Reina MA, Machés F, Hernández JM, De Andrés J, van Zundert A. 2011. Three-dimensional magnetic resonance image of structures enclosed in the spinal canal relevant to anesthetists and estimation of the lumbosacral CSF volume. Acta Anaesthesiol Belg 62:37-45.

Reina MA, Arriazu R, Collier CB, Sala-Blanch X. 2013. Histology and electron microscopy of human peripheral nerves of clinical relevance to the practice of nerve blocks. Rev Esp Anestesiol Reanim 60:552-562.

Reina MA, Sala-Blanch X, Fernández P. 2015a. Cross-sectional microscopic anatomy of dissected sciatic nerve. In: Reina MA, editor. Atlas of Functional Anatomy of Regional Anesthesia and Pain Medicine. New York: Springer. p 213-236.

Reina MA, Sala-Blanch X, Arriazu R, Machés F. 2015b. Microscopic morphology and ultrastructure of human peripheral nerves. In: Tubbs RS, Rizk E, Shoja M, Loukas M, Spinner RJ, Barbaro N, editors. Nerves and Nerve Injuries, Vol. 1. San Diego CA: Academic Press-Elsevier. p 91-106.

Reina MA, Lirk P, Puigdellívol-Sánchez A, Mavar M, Prats-Galino A. 2016. Flavum anatomy for epidural anesthesia: reviewing a 3D MR-based interactive model and postmortem samples. Anesth Analg 122:903-907.

Sala-Blanch X, Ribalta T, Rivas E, Carrera A, Gaspa A, Reina MA, Hadzic A. 2009. Structural injury to the human sciatic nerve alter intraneural needle insertion.

Reg Anesth Pain Med 34:201-205.

Sala-Blanch X, Vandepitte C, Laur J, Horan P, Xu D, Reina MA, Hadzic A. 2011a. Practical review of perineural versus intraneural injections: a call for standard nomenclature. International Anesthesiology Clinics 49:1-12.

Sala-Blanch X, Lopez AM, Pomes J, Valls-Sole J, Garcia AI, Hadzic A. 2011b. No clinical or electrophysiologic evidence of nerve injury after intraneural injection during sciatic popliteal block. Anesthesiology 115:589-595.

Sala-Blanch X, Reina MA, Ribalta T, Prats-Galino A. 2013. Sciatic nerve structure and nomenclature: epineurium to paraneurium Is this a new paradigm? Reg Anesth Pain Med 38:463-465.

Sharpe J. Optical projection tomography as a new tool for studying embryoanatomy. J Anat. 2003; 202:175-181.

Sunderland S. 1945. The intraneural topography of the radial, median and ulnar nerves. Brain 68:243-255.

Sunderland S, Bradley KC. 1949. The cross-sectional area of peripheral nerve trunks devoted to nerve fibres. Brain 72:428-449.

Sunderland S, Marshall RD, Swaney WE. 1959. The intraneural topography of the circumflex musculocutaneous and obturator nerves. Brain 82:116-129.

Sunderland S, Ray LJ. 1948. The intraneural topography of the sciatic nerve and its popliteal divisions in man. Brain 71:242-258.

Tainaka K, Kuno A, Kubota SI, Murakami T, Ueda HR. 2016. Chemical principles in tissue clearing and staining protocols for whole-body cell profiling. Ann Rev Cell Dev Biol 32:713-741.

FIGURES

Figure 1. Optical projection tomography images of the median nerve in axial, sagittal and coronal sections. The perimeters of fascicles are delimited in red, green and blue colors.

Figure 2. 3D reconstruction of fascicles of the median nerve. a - The fascicles are not rectilinear; instead we can see waves of them. b - 3D reconstruction technique allowed

fascicles to be clearly delineated. The assigned color helps us to identify details of each.

Figure 3. 3D reconstruction of fascicles of the lingual nerve. a - The fascicles are rectilinear, in contrast to Fig. 2, and do not have waves. b - 3D reconstruction with assigned color helps us to identify details of each.

Figure 4. 3D reconstruction of fascicles of the median nerve. a - Details of the waves with isolated fascicle pattern; a single nerve fascicle with no relationship to adjacent fascicles. b - A bifurcation or "inverted Y-shape" pattern.

Figure 5. 3D reconstruction of fascicles of median nerve. a - Details of two fascicles with a confluence or "Y-shape" pattern, in which two fascicles usually converge to form a single fascicle. b – Detail of two fascicles crossing or "X-shape" pattern.

Figure 6. 3D reconstruction of fascicles of the median nerve. a - Two fascicles are connected to a little fascicle. The fascicular interconnection, a thin bridge between two nerve fascicles. b - complex interconnection, resulting from a variable combination of previous patterns in the segment of nerve analyzed.

The authors declare no conflicts of interest.

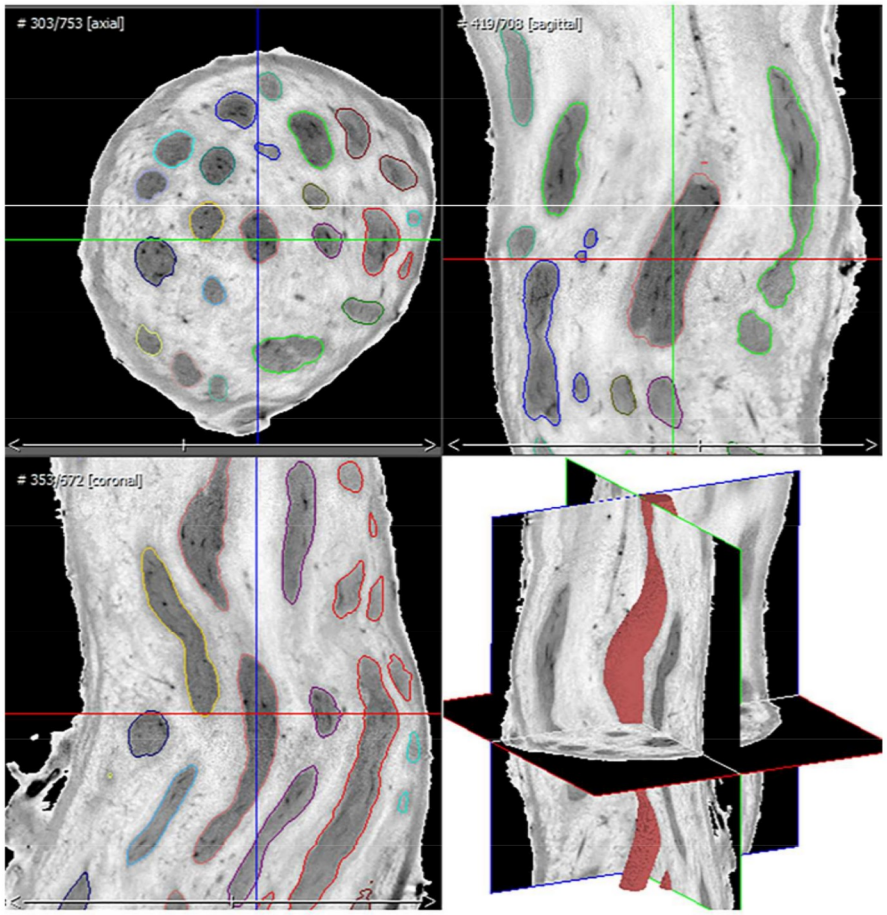

190x254mm (300 x 300 DPI)

190x254mm (300 x 300 DPI)

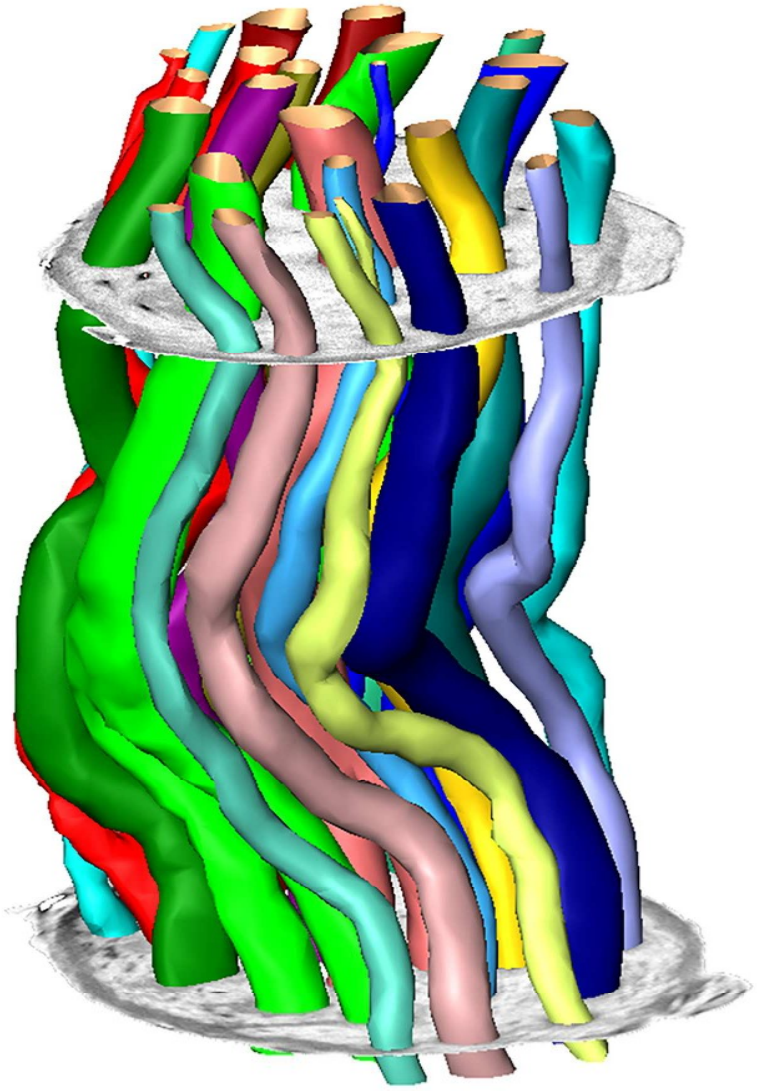

190x254mm (300 x 300 DPI)

190x254mm (300 x 300 DPI)

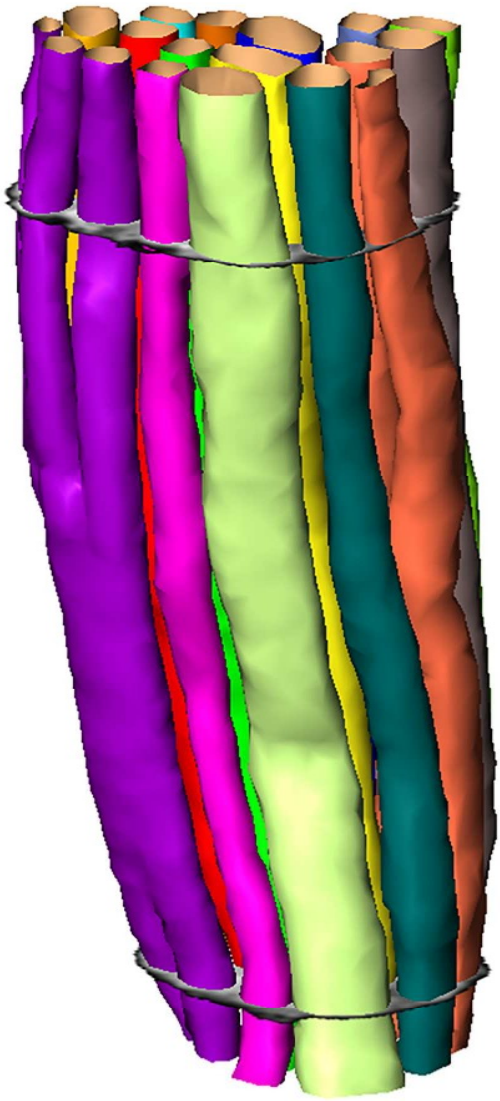

190x254mm (300 x 300 DPI)

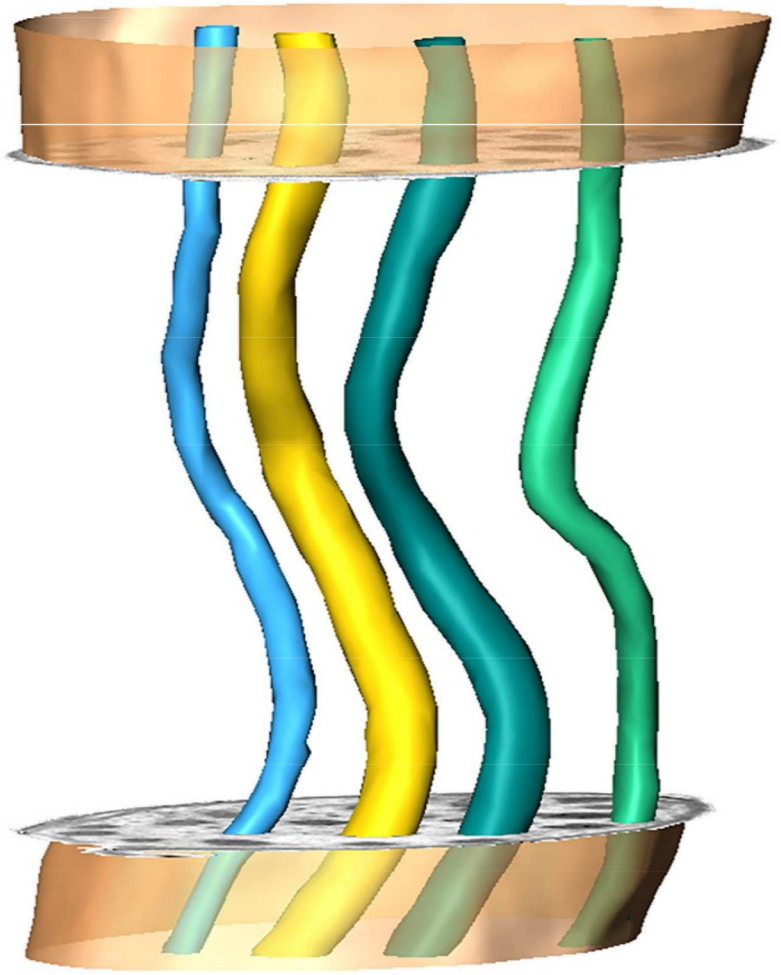

190x254mm (300 x 300 DPI)

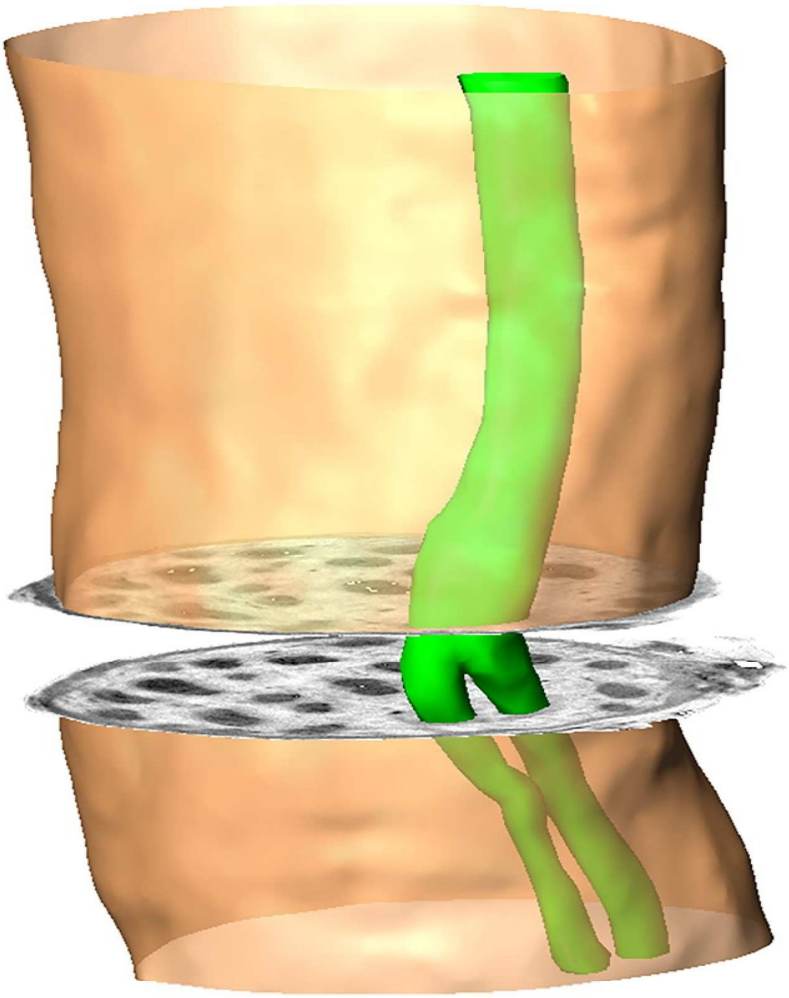

190x254mm (300 x 300 DPI)

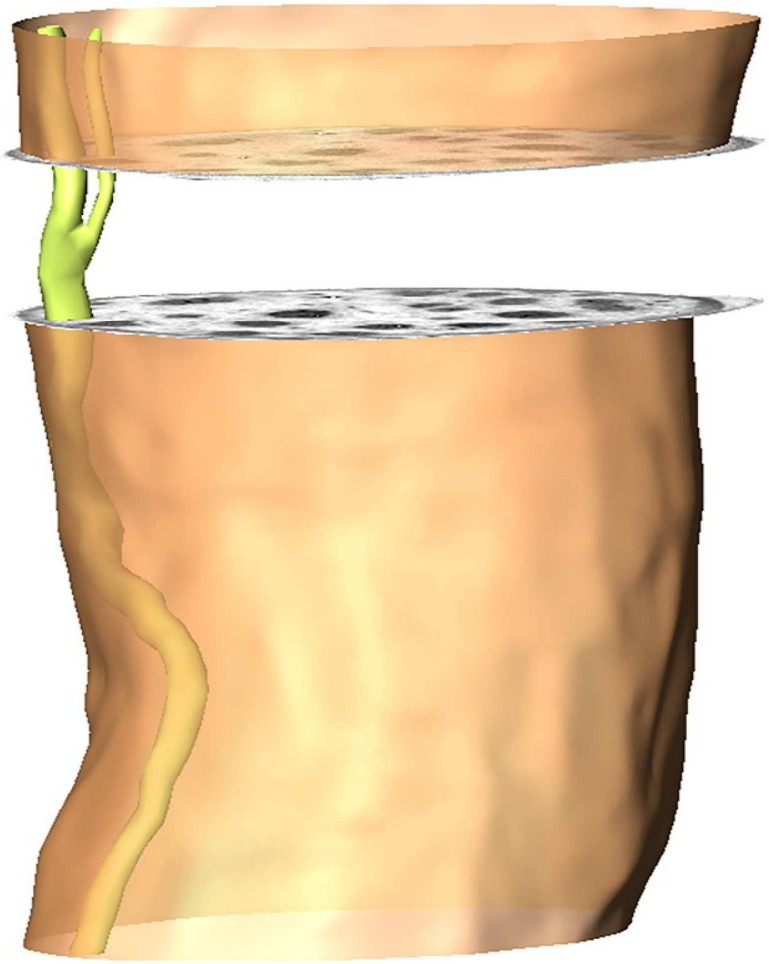

190x254mm (300 x 300 DPI)

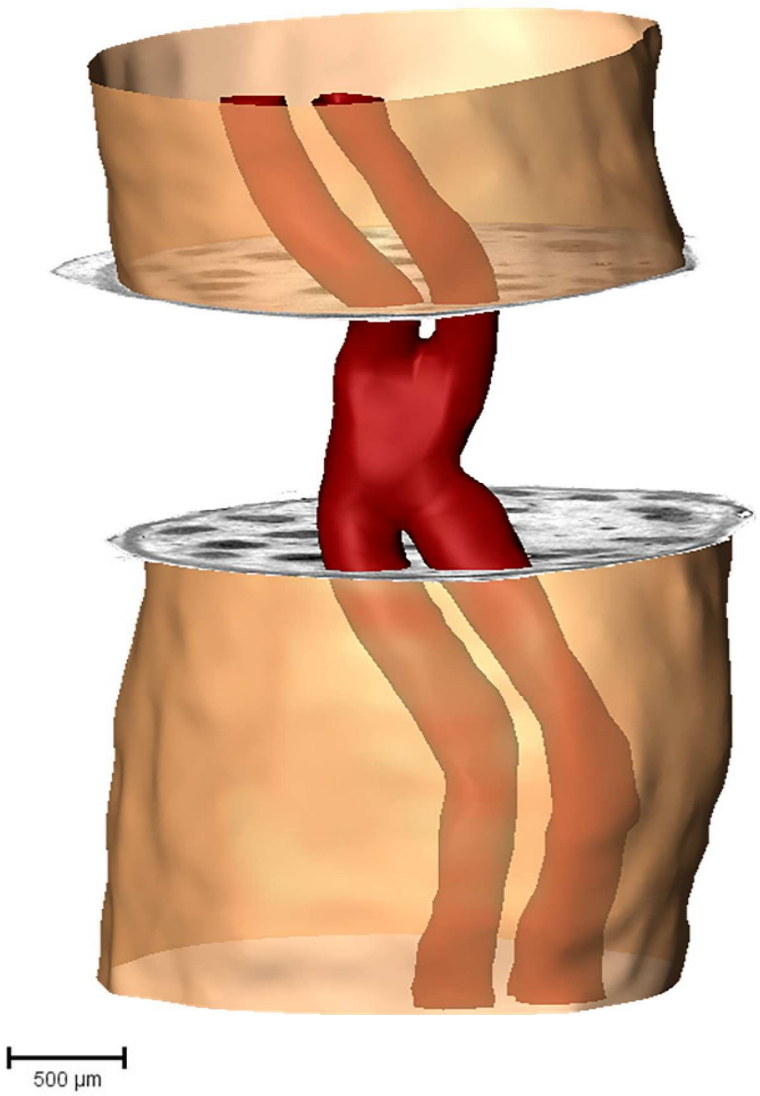

190x254mm (300 x 300 DPI)

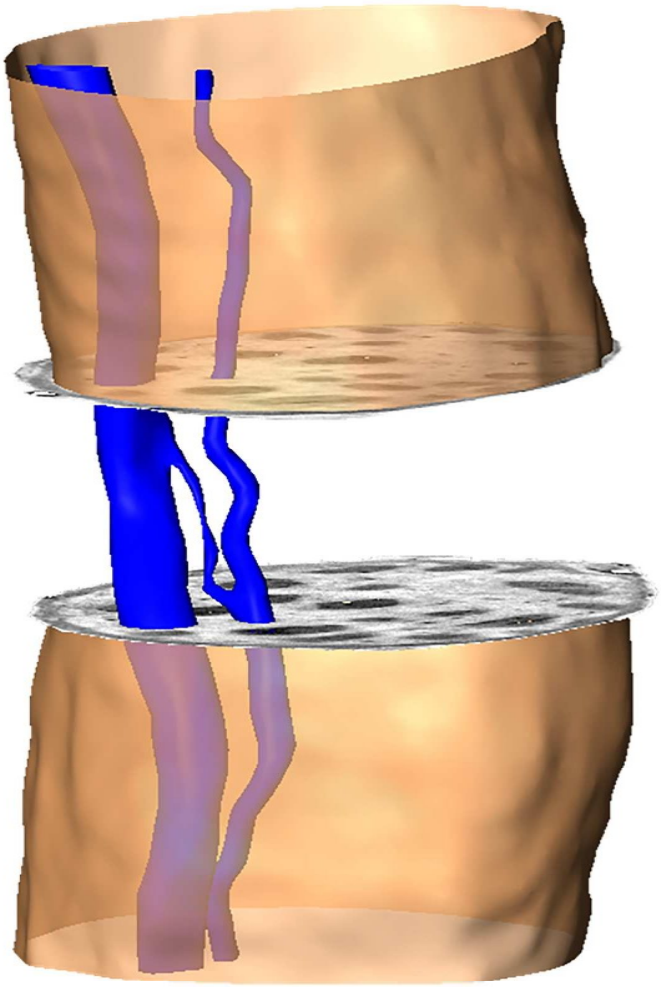

190x254mm (300 x 300 DPI)

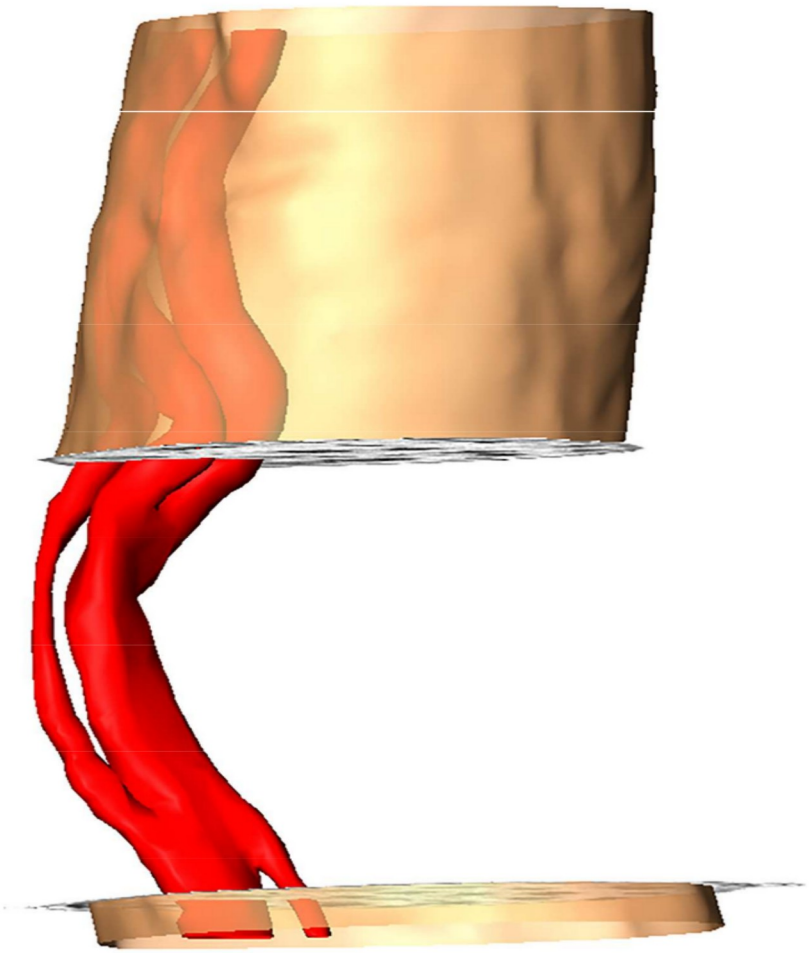

190x254mm (300 x 300 DPI)